Anisotropy of diffusion in a liquid crystalline system of semi-flexible polymer chains

ARTICLE *in* PHYSICAL CHEMISTRY CHEMICAL PHYSICS · JUNE 2003

Impact Factor: 4.49 · DOI: 10.1039/b300615h

5 AUTHORS, INCLUDING:

A. A. Darinskii
Russian Academy of Sciences
98 PUBLICATIONS **731** CITATIONS
SEE PROFILE

Nikolay K. Balabaev
Russian Academy of Sciences
133 PUBLICATIONS **948** CITATIONS
SEE PROFILE

Igor Neelov
68 PUBLICATIONS **461** CITATIONS
SEE PROFILE

PCCP

Anisotropy of diffusion in a liquid crystalline system of semi-flexible polymer chains

Anatoly A. Darinskii,[a] Anna Zarembo,*[b] Nikolai K. Balabaev,[c] Igor M. Neelov[abd] and Franciska Sundholm[b]

[a] *Institute of Macromolecular Compounds, Bolshoi pr.31, 199004, St.-Petersburg, Russia. E-mail: adar@imc.macro,ru; Fax: +7 812 3286869; Tel: +7 812 3285601*
[b] *Laboratory of Polymer Chemistry, University of Helsinki, P.O.Box 55, FIN-00014 Helsinki, Finland. E-mail: anna.zarembo@helsinki.fi; Fax: +358 19150 330; Tel: +358 191 50 346*
[c] *Institute of Mathematical Problems of Biology, 142292, Pushchino, Russia. E-mail: balabaev@impb.psn.ru; Fax: +7 0967 790570*
[d] *University of Leeds, IRC in Polymer Science and Technology, Leeds, UK LS2 9JT. E-mail: neelov@csc.fi*

Received 16th January 2003, Accepted 7th April 2003
First published as an Advance Article on the web 24th April 2003

Molecular dynamic simulations are reported for semi-flexible systems consisting of rod-like linear molecules. The molecules are composed of eight tangent isotropic soft spheres, connected by continuous elastic springs into a linear chain. Rigidity is introduced by additional springs between each sphere along the chain. The elasticity of the springs is used to tune the flexibility of the molecule. The formation of only a nematic LC phase is shown for all systems considered. Persistence length dependences of the jump of the order parameter and boundary volume fractions in isotropic and nematic phases at LC transition agree well with predictions of the Khokhlov–Semenov theory and with available simulation data. The effect of the flexibility on the translational and rotational diffusion in the nematic phase is studied. The anisotropy of translational diffusion was observed. For the estimation of the rotational diffusion coefficient for molecules in a nematic phase the wobbling-in-a-cone model was applied. Anisotropy of translational diffusion and ratio of translational and rotational diffusion coefficients show universal dependences on the order parameter.

1. Introduction

Liquid crystals (LC) have many applications due to their unique combination of solid and liquid properties. It is well known that solutions of molecules with a sufficiently anisotropic shape can form a lyotropic LC phase at definite concentrations.[1] One of the most interesting dynamical properties is self-diffusion anisotropy of molecules in the LC phase. There are several publications devoted to the theoretical and simulation studies of molecule mobility in such systems (see for example refs. 2–7). The majority of these publications consider models of rigid anisotropic particles. In particular Allen[7] has simulated dense systems of prolate and oblate hard ellipsoids with different axis ratio. His results were explained on the base of an affine transformation model.[8] Lowen has performed a Brownian dynamics simulation of a concentrated solution of hard spherocylinders[5] with a different shape anisotropy. It was shown that the ratio of self-diffusion coefficients along and normal to the director D_{par}/D_{per} essentially depends on the nematic order parameter alone.

Many real LC systems consist of semi-flexible molecules. In particular the flexibility plays an important role in the statistical physics of liquid crystalline polymers.[9,10] Semiflexible LC polymers show a wide variety of phase behaviour and play the important role in biology and material science.[11] Most of the theoretical and simulation works devoted to semi-flexible LC macromolecules were focused on the structure of the ordered phase, the location of the LC transition on the density scale and change of the order parameter in the transition region. All theories (see reviews[10,12]) predict a LC transition for sufficiently long molecules with the definite flexibility by increase of the volume fraction of polymer. The concentration at which LC transition takes place shifts to larger values for more flexible molecules Theoretical predictions are confirmed by computer simulations.[2,13–16]

Far less studied are dynamical properties of semi-flexible molecules in the LC phase. As usual the possibilities of the analytical theory in this field are very restricted and computer simulation occurs to be a powerful tool to study these properties. Up to now the self-diffusion in the ordered phase for semi-flexible molecules was studied only in the unpublished work of Kolb[2] by the method of molecular dynamics (MD). The chain model used consisted of soft particles interacting with purely repulsive modified Lennard-Jones potentiales. The rigidity was introduced through the local bending potential depending on the angle between adjacent bonds. The anisotropy of diffusion in the nematic and smectic phases was demonstrated and used as one of the indicators of type of the LC phase. But the systematic analysis of effect of the flexibility on the anisotropic diffusion was not reported.

In our recent study[3] we have simulated a slightly different semi-flexible model by the MD method, also consisting of isotropic soft particles with purely repulsive interactions and connected into the chain by elastic springs. In contrast to model[2] the rigidity was introduced into the model through additional springs connecting nonadjacent beads. The flexibility was regulated by the change of elastic constants of springs. In ref. 3 the chains consisting of different number of particles $N_c = 6,7,8$ but only with the same moderate flexibility were simulated. The formation of the nematic LC phase and the anisotropy

 DOI: 10.1039/b300615h

of self-diffusion in this phase was observed only for $N_c = 8$. In the present work we consider the same model with $N_c = 8$ but we vary the flexibility. Our main goal is to study the effect of the flexibility on the chain dynamics in the LC state.

The plan of the paper is the following. In section 2 we describe the model, methods of preparation and simulation of our system. Section 3 contains results concerning the phase behavior of the system. In section 4 the dynamic properties are discussed. Section 5 concludes the paper.

2. Model and method of simulation

We use as a model a semiflexible rod-like linear molecule, consisting of N_c Lennard-Jones (LJ) particles. All particles in the system interact according to a truncated LJ 6–12 potential U_{LJ}, which corresponds to pure repulsive interactions between the particles in the system:

$$\begin{aligned} U &= U_{LJ}(r) - U_{LJ}(R), & r \le R \\ &= 0, & r > R \end{aligned} \tag{1}$$

where r is the distance between the particles, R-the radius of truncation.

$$U_{LJ} = 4\varepsilon((\sigma/r)^{12} - (\sigma/r)^{6}) \tag{2}$$

The LJ potential parameters σ and ε are equal to 1.0, $R = 2^{1/6}$.

Rigidity of the molecule is introduced by Frenkel springs between all particles along the chain. The elastic energy per molecule is:

$$U_{el} = \sum_{s=1}^{N_c-2} \sum_{i=s+2}^{N_c} U_{si}, \tag{3}$$

where the potential of the spring between the ith and sth particles is given by the formula

$$U_{si} = \frac{K_{si}}{2}(|r_s - r_i| - (s-i)l_0)^2 \tag{4}$$

where l_0 is the equilibrium bond length assumed $l_0 = \sigma$, s is the number of neighbour particle along the chain. Such a method of controlling of the rigidity is close to that in ref. 11 where the hard-wall potentials were used to bind adjacent as well as more remote hard spheres together. The allowed bond length fluctuations provide the certain chain flexibility. In our model constrains are imposed not by hard wall potentials but by continuous elastic springs, which connect all particles in the molecule. Instead of the hard sphere model we used soft repulsive potentials between chain particles. In this relation our model has common features with model.[2] In the present study we consider the model in which all springs (including the bond length one) have the same elasticity constant K_s. The layout of the model is shown in Fig. 1. In our previous work[3] we studied only the case of the moderate spring elasticity $K_s = 50$ for different N_c. In the present work we vary K_s at the constant number of particles in the chain $N_c = 8$. Three systems with the spring elasticity $K_s = 50$, 100 and 500 (in reduced units) were considered.

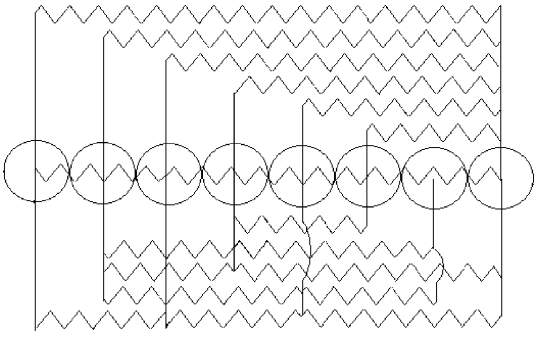

Fig. 1 Layout of the model mesogen $N_c = 8$.

The simulation was performed by the molecular dynamics method using the Verlet algorithm[17] for the numerical integration of equations of motion. All simulated systems contained $N_m = 1536$ molecules in the simulation box. The reduced units for time $\tau = \sigma(m/\varepsilon)^{1/2}$ and length σ were used as usual. The integration step $\Delta t = 0.004$ was selected. All calculations were performed at the same temperature $T = 0.5/k_B$ where k_B is the Boltzmann constant.

As an initial structure a regular completely ordered array of molecules on a simple cubic lattice with number density $\rho = N_m N_c/V = 1$ was used. Molecules were aligned parallel to the long axis OZ of the simulation cell. We will denote this ordered structure as a crystal state. The X and Y dimensions of the cell were equal to 16 to avoid the intersections of images of molecules in neighbouring cells. The system consisted of six layers along the OZ direction and size of the cell in this direction was equal to $6N_c$. To obtain systems with smaller densities the systems were equilibrated at the constant temperature and pressure (NPT ensemble) at different external pressures. The Berendsen procedure[18] for NPT ensemble was used. The equilibrium state was considered being achieved after the density and order parameter become stable on a sufficiently long part of the trajectory. After this equilibration run static and dynamical characteristics of the systems were calculated using NVT ensemble (the constant temperature and volume). The lengths of the equilibration and productive runs were about 5×10^6 and 3×10^3 time steps correspondingly The calculations were carried out using computer time provided by Centre of Scientific Computing (CSC, Espoo, Finland), and took about 3300 CPU hours on Cray T3E or 1200 CPU hours on Origin 2000 SGI computers.

3. Static characteristics. Phase behavior

The order parameter S was determined as

$$S = \frac{3}{2}\left\langle \cos^2\theta - \frac{1}{3}\right\rangle, \tag{5}$$

where θ is the angle between the end-to-end vector $\boldsymbol{a}_j$ of the molecules and the director.

The calculated dependences of the order parameter S on the density are shown in Fig. 2. Step-like increase of S in the narrow density region is observed for all systems. The curves shift

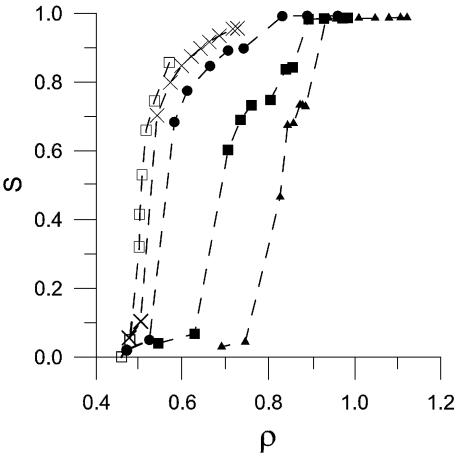

Fig. 2 Order parameter dependence of density for systems considered. Triangles: $l_p = 132$, filled squares: $l_p = 199$, filled circles: $l_p = 430$, crosses: Kolb results, open squares: Yethiraj and Fynewever results.

to larger values of density with the increase of the flexibility. We plot also the data for the Kolb model[2] (persistence length $l_p = 1000$) and for that of Yethiraj and Fynewever[15] (infinite l_p) for the chains with $N_c = 8$.

For estimation of values of persistence length for our model one can use the formula of mean square end-to-end distance $\langle h^2 \rangle$ for persistence chain model derived for short chains $L/l_p \ll 1$[19]

$$\langle h^2 \rangle = L^2 \left[1 - \frac{1}{3}\frac{L}{l_p} + \frac{1}{12}\left(\frac{L}{l_p}\right)^2 \right] \quad (6)$$

where $L = (N_c - 1)l_0$ is the contour length of the chain, l_0 is the equilibrium length of the bond. For our model we obtain the following persistent lengths: for $K_s = 50$ $l_p = 132$, for $K_s = 100 l_p = 199.7$, for $K_s = 500$ $l_p = 430.4$. The $\langle h^2 \rangle$ values corresponding to maximum density of isotropic phases of each system were used for calculation of l_p.

Analysis of our simulation data shows that the ordered phase with the order parameter $S = 0.6$–0.9 corresponds to the nematic state. At larger densities the transition into crystalline state is observed. Snapshots (Fig. 3) confirm this conclusion. We have not observed the formation of the smectic phase even in case of the most rigid chains. The position of the nematic–isotropic (N–I) transition was determined from the dependence of S on density, as a region where S starts to drops abruptly. It is shifted to smaller values of density as K_s increase.

To compare our results with the theory predictions it is good to bear in mind that the theory connects the jump of the order parameter ΔS and volume fractions of isotropic Φ_i and nematic phases Φ_n at the I–N transition with ratio L to l_p.

The most simple Khokhlov–Semenov theory[9] uses the second virial expansion for a hard wormlike cylinder model with the diameter d. Strictly speaking it is applicable to polymer solutions. In our case we have a rather dense system where the solvent is absent. For our case $L/l_p \ll 1$ the Khokhlov–Semenov theory predicts the following dependences of ΔS, Φ_n and Φ_i on L, l_p and d:

$$\Delta S = 0.847 - 1.487 L/l_p \quad (7)$$

$$\Phi_i = 3.34 d/L + 4.99 d/l_p \quad (8)$$

$$\Phi n = 4.486 d/L - 1.458 d/l_p \quad (9)$$

There is some ambiguity in the definition of the volume occupied by the molecule with the soft interaction potential in eqn. (1). Considering our molecules as cylinders with diameter $d = \sigma$ and length $L = (N_c - 1)\sigma$ we can determine the volume occupied by a single molecule $\nu = d^2\pi/4L$ and the volume fraction of the polymer in the system $\Phi = \nu\rho/N_c$. The values of the jump of the order parameter ΔS and the volume fractions Φ_n were determined as corresponding values in the points on the curves in Fig. 2, where curves remarkably

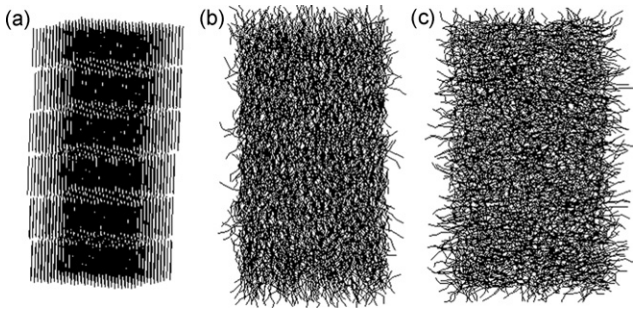

Fig. 3 Typical snapshots of three states of the simulated systems: (a)-completely ordered state (isometry), (b)-LC state (XZ plane), (c) isotropic state (XZ plane).

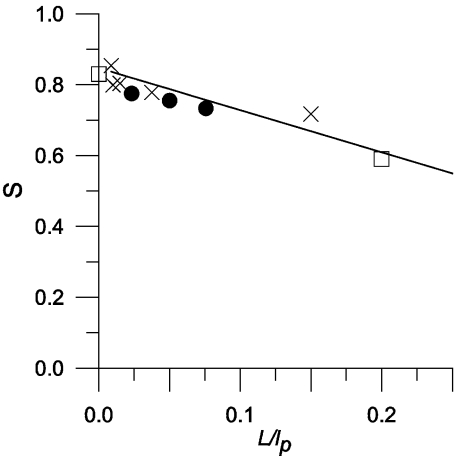

Fig. 4 Order parameter S at isotropic-nematic transition *vs.* ratio of chain length L to its persistence length l_p. Solid line: Khokhlov–Semenov theory, circles: our simulation results, crosses: Kolb results, squares: Yethiraj and Fynewever results.

change their slopes before the transition to the isotropic state. The values of Φ_i correspond to the points on these curves where their slopes change again at values of S close to zero. The similar procedure was used to estimate these characteristics from the data, reported by Yethiraj and Fynewever[15] and Kolb.[2]

In Fig. 4 and 5 one can see that our simulated values of ΔS and Φ_i, Φ_n as well as those obtained from Kolb's and Yethiraj and Fynewever's data are in satisfactory agreement with theory predictions taking into account some uncertainty by fitting of parameters of the many particle models to those of hard wormlike cylinder model and the accuracy of the theory.[10]

4. Dynamic properties

4.1. Translational self-diffusion

It is known that nematic LC exhibits a dynamical anisotropy: the self-diffusion of molecules along the director is easier than that in the normal direction.

To investigate how this property depends on the chain flexibility we have calculated the time dependencies of the mean square displacements of centres of mass of the molecules along the axis of regularity $\langle \Delta r^2_{par}(t) \rangle$ and in the perpendicular direction $\langle \Delta r^2_{per}(t) \rangle$ (see Fig. 6). The diffusion coefficients D_{par} and

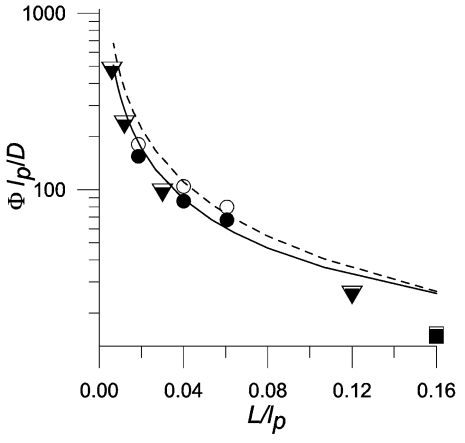

Fig. 5 Scaled isotropic (I) and nematic (N) volume fractions at the phase transition *vs.* L/l_p: open symbols correspond to (N) phase, filled-to (I) one. Circles: our simulation results, triangles: Kolb results, squares: Yethiraj and Fynewever results. Khokhlov–Semenov theory results plotted by lines, dashed: (N) phase, solid: (I) phase.

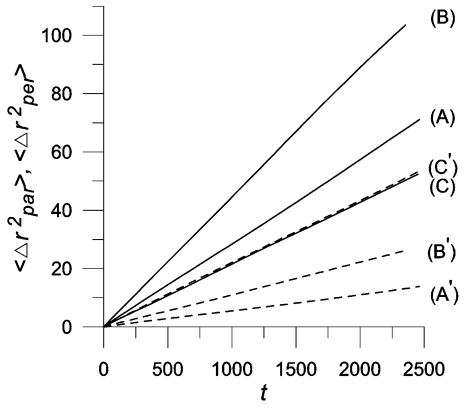

Fig. 6 Mean square displacement along the director $\langle \Delta r^2_{\mathrm{par}} \rangle$ (solid lines) and in a perpendicular plane $\langle \Delta r^2_{\mathrm{per}} \rangle$ (dashed lines) dependence of time for selected phases of system with $l_{\mathrm{p}} = 430$. (A) nematic phase with $S = 0.885$, (B) nematic phase with $S = 0.77$ and (C) isotropic phase $S = 0.04$.

D_{per} were calculated from the slopes of corresponding curves, using $\langle \Delta r^2_{\mathrm{par}}(t) \rangle = 2D_{\mathrm{par}}t$ and $\langle \Delta r^2_{\mathrm{per}}(t) \rangle = 2D_{\mathrm{per}}t$

Following ref. 5 we can also define ''isotropic'' value of the self-diffusion coefficient

$$D = (2D_{\mathrm{per}} + D_{\mathrm{par}})/3 \tag{10}$$

Simulated values of D, D_{par} and D_{per} are given in the Table 1.

The dependences of D, D_{par} and D_{per} on the density are shown on Fig. 7a,b,c for three systems with different parameters of flexibility l_{p}. In the isotropic phase the anisotropy of diffusion disappears. In the nematic phase the diffusion coefficient along the director D_{par} behaves nonmonotonically with ρ. The maximum of D_{par} is shifted to smaller densities for more rigid chains. Its value increases with increase of rigidity. The nonmonotonic behaviour of D_{par} with density was observed first by Allen for the dense system of hard ellipsoids[7] and later by Lowen[5] for the concentrated solution of hard spherocylinders.

The value of the anisotropy of diffusion can be characterized by the ratio $D_{\mathrm{par}}/D_{\mathrm{per}}$. Simulated values of this ratio are given in the Table 1. Its dependences on the density for three systems are shown in Fig. 8. We do not observe any anisotropy in the crystal and isotropicphases but rather a large one in the LC state. The more flexible system has the lower diffusion anisotropy. Its density dependence is nonmonotonic. The maximum value of $D_{\mathrm{par}}/D_{\mathrm{per}}$ varied from 3.3 for the system with $l_{\mathrm{p}} = 132$ to 5.7 for the system with $l_{\mathrm{p}} = 430$.

Table 1 Parameters of translational diffusion

lp	ρ	S	$D \times 10^3$	$D_{\mathrm{par}} \times 10^3$	$D_{\mathrm{per}} \times 10^3$	$D_{\mathrm{par}}/D_{\mathrm{per}}$
132	0.879	0.733	2.11	4.06	1.23	3.29
132	0.872	0.734	2.32	4.40	1.30	3.38
132	0.844	0.675	2.84	5.29	1.66	3.18
132	0.746	0.041	3.90	3.90	3.88	1.01
199.7	0.840	0.832	2.73	6.50	0.84	4.95
199.7	0.804	0.814	4.02	8.71	1.80	4.83
199.7	0.76	0.762	5.07	10.65	2.58	4.12
199.7	0.703	0.578	6.34	10.13	3.79	2.93
199.7	0.625	0.04	7.25	7.16	7.29	0.98
430.4	0.742	0.909	4.91	10.82	2.05	5.26
430.0	0.706	0.885	6.75	14.57	2.89	5.03
430.4	0.664	0.842	8.45	17.45	4.04	4.32
430.4	0.611	0.770	11.18	22.18	5.61	3.96
430.4	0.581	0.684	11.09	20.19	6.55	3.08
430.4	0.523	0.040	11.02	10.60	10.91	0.98

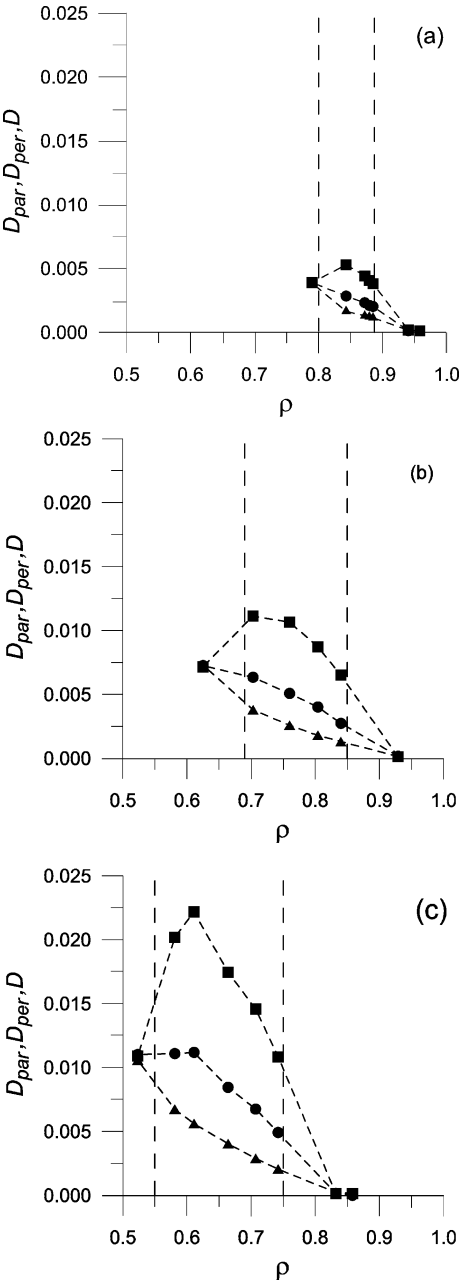

Fig. 7 Diffusion coefficients as function of density; squares: D_{par}, triangles: D_{per}, circles: D for the systems of different flexibility: (a) $l_{\mathrm{p}} = 132$, (b) $l_{\mathrm{p}} = 199$, (c) $l_{\mathrm{p}} = 430$. The lines are a guide to the eye. The vertical dashed lines indicate, from left to right, the isotropic region, the nematic region and the crystal region.

In ref. 5 it was shown that for the concentrated solution of spherocylinders the anisotropy of diffusion is essentially dependent on the nematic order parameter alone. The theoretical upper limit for this ratio

$$D_{\mathrm{par}}/D_{\mathrm{per}} \approx \frac{2S+1}{1-S} \tag{11}$$

was obtained by assumption of motion only in the direction parallel to the orientations of molecules.[5]

In Fig. 9 we plot our simulation results for $D_{\mathrm{par}}/D_{\mathrm{per}}$ *versus* S. Lowen's data[5] are also shown. All simulation data reasonably fall on a single curve. At the isotropic-nematic transition $D_{\mathrm{par}}/D_{\mathrm{per}} \approx 3$. This value is consistent with $2 < D_{\mathrm{par}}/D_{\mathrm{per}} < 4$ obtained in ref. 5 at the point of transition as well as with experimental data for colloidal solution of boehmite rods.[6]

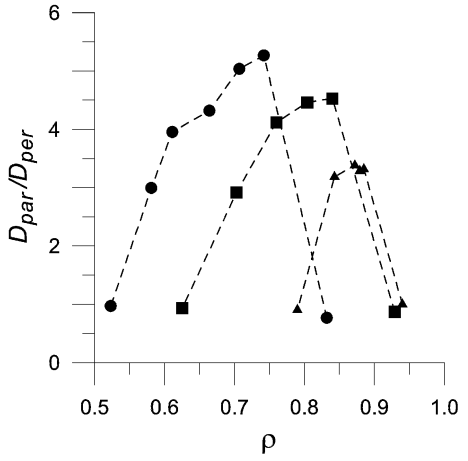

Fig. 8 Diffusion anisotropy at different density for the systems with different flexibility. Triangles: $l_p = 132$, squares: $l_p = 199$, circles: $l_p = 430$. The lines are a guide to the eye.

Therefore the conclusion made in ref. 5 for nematic LC consisting of rigid rod-like molecules that the anisotropy of diffusion is a function of S alone is of more universal character and is valid also for semi-flexible molecules.

Such an universality is not observed for the ellipsoids. It was shown[8] that in this case the ratio D_{par}/D_{per} is a function not only of the order parameter S but also of the axis ratio Q

$$D_{par}/D_{per} = Q^2\ ((1 + 2/3(Q^{-2} - 1)(1 - S))/ ((1 + 1/3(Q^2 - 1)(1 - S)) \quad (12)$$

This formula turns into eqn. (11) at $Q = \infty$.

The anisotropy of diffusion can be characterized also by the parameter R

$$R = (D_{par} - D_{per})/(D_{par} + 2\ D_{per}) \quad (13)$$

For ellipsoids in the nematic phase the linear dependence of parameter R on S with slope dependent on the axis ratio Q was observed:[8]

$$R = (Q^2 - 1)/(Q^2 + 2)\ S \quad (14)$$

In Fig. 10 we plot the values of R calculated from our and Lowen's data against S. We see that for rod-like particles (rigid and semi-flexible) the $R(S)$ dependence is close to linear but we do not see any remarkable dependence of its slope on the aspect ratio p and flexibility.

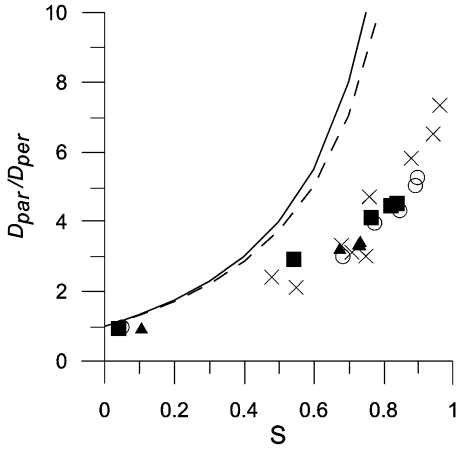

Fig. 9 Diffusion anisotropy in a nematic and isotropic phase as a function of order parameter S for the systems with different flexibility. The solid line is the theoretical upper bound according to eqn. (11), dashed line is according to eqn. (12), triangles: $l_p = 132$, squares: $l_p = 199$, open circles: $l_p = 430$. The results of Lowen[5] are given by crosses.

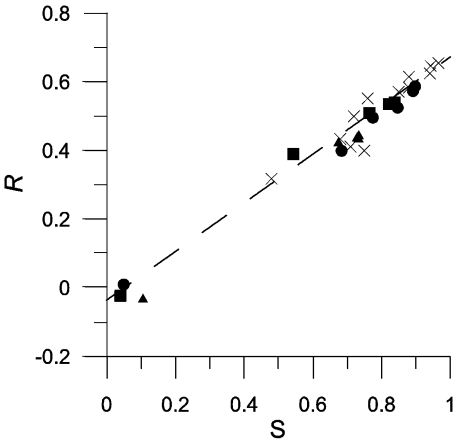

Fig. 10 Diffusion anisotropy according eqn. (14) in a nematic and isotropic phase as a function of order parameter S for the systems with different flexibility. Triangles: $l_p = 132$, squares: $l_p = 199$, circles: $l_p = 430$. The results of Lowen[5] are given by crosses. The dashed line is the best fit for all data.

4.2. Orientational mobility of molecules

For characterization of the orientational mobility the orientation correlation functions

$$P_1 = \langle \cos\theta(t) \rangle \quad \text{and} \quad P_2 = \frac{3}{2}(\langle \cos^2\theta(t) \rangle - 1/3) \quad (15)$$

where calculated. $\theta(t)$ is an angle of rotation of the long axis for the time t.

For the rotational diffusion of the rigid particle in a viscous medium

$$P_2(t) = P_1^3(t) \quad (16)$$

and

$$P_2(t) = \exp(-6D_{rot}t) \quad (17)$$

where D_{rot} is the rotational diffusion coefficient.The Fig. 11 shows the exponential decay of the function $P_2(t)$ in an isotropic phase for all flexibilities considered and proves the correctness of eqn. (16) for our case.

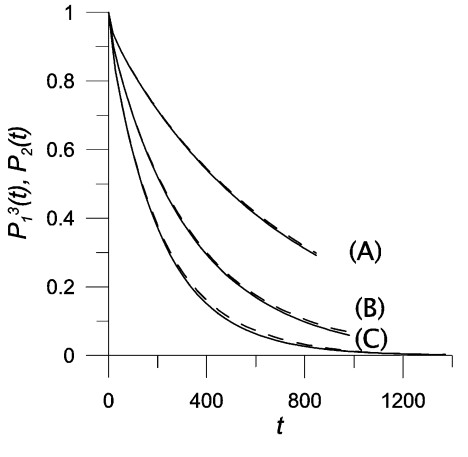

Fig. 11 The correlation functions $P_2(t)$ (solid line) and $P_1^3(t)$ (dashed line) for an isotropic phase as a function of time for all flexibilities. (A) $l_p = 132$, (B) $l_p = 199$, (C) $l_p = 430$.

Table 2 Rotational diffusion coefficient D_{rot} and ratio D/D_{rot} in the isotropic phase for systems simulated

l_p	ρ	$10^3 D_{rot}(S=0)$	$D(S=0)/D_{rot}(S=0)$
132	0.746	0.226	17.3
199.7	0.625	0.468	15.5
430.4	0.523	0.738	14.9

For diffusion of rigid cylinders in the homogeneous solvent the following analytical expressions were obtained:[20]

$$D_{rot} = \frac{3D_0}{\pi L^2}(\ln p - 0.662 + 0.917/p - 0.050/p^2) \quad (18)$$

$$D = \frac{D_0}{3\pi}(\ln p + 0.312 + 0.565/p - 0.100/p^2) \quad (19)$$

with $D_0 = k_B T/\eta L$, where η is the shear viscosity of the solvent, L is length of the cylinder and p is aspect ratio.

By using values of $p = 8$ and $L = 8$ for our system we obtain the theoretical value $D/D_{rot} = 11.5$.

Simulated values of the rotational diffusion coefficient D_{rot} as well as the ratio D/D_{rot} in the isotropic phase are given in the Table 2.

We see that values D/D_{rot} decrease with increase of the rigidity of the molecule but remain larger than the theoretical value. The full agreement can not be expected due to the difference between our semiflexible model and hard cylinders.

Nevertheless the closeness of the simulated data to theoretical prediction for rigid cylinders in a viscous medium allows to conclude that the effect of surrounding molecules on the diffusion of selected molecule in our system is equivalent to the effect of some homogeneous solvent.

In the nematic state the correlation functions $P_1(t)$ and $P_2(t)$ do not decay to zero. The rotational motions of molecules in this state can be considered as a restricted rotational diffusion. For the analysis of our data a wobbling in a cone model can be applied.[21] In this model the rotational diffusion of a particle assumed to be free within a cone of semiangle θ_0 and forbidden on the outside. The value of θ_0 can be estimated from the equation:

$$\cos\theta_0(1 + \cos\theta_0) = 2S \quad (20)$$

For $P_2(t)$ a semi-empirical expression can be used:

$$P_2(t) = (1 - P_2(\infty))\exp(-t/t_r) + P_2(\infty) \quad (21)$$

where $t_r = \sigma_r/D_{rot}$ and σ_r depends solely on θ_0 *i.e.* on S. For restricted rotational diffusion $P_2(\infty) = S^2$.

In ref. 21 the rotational diffusion of an anisotropic Brownian particle within a cone of different semiangles θ_0 was simulated and the dependence of σ_r on S was calculated. We assume that rotation in a nematic phase can be considered as a restricted diffusion with $D_{rot}(S)$ in a cone with the semiangle θ_0 determined by eqn. (20).

Fig. 12 shows the simulated time dependences of $\ln(P'_2(t)) = \ln((P_2(t) - S^2)/(1 - S^2))$ for the most rigid system with $l_p = 430$ as an example. Some curvature is observed indicating the deviation from pure exponential decay but it is not much pronounced. Following ref. 21 we have obtained t_r values (Table 3) from the straight line that best fits the point of the central part of the decay, chosen as $0.8 \geq ((P_2(t) - S^2)/(1 - S^2)) \geq 0.2$.

Using these values of t_r we have calculated $D_{rot}(S)$(Table 3).

It is instructive to calculate the ratio D/D_{rot} where D is given by eqn. (10). The use of this ratio allows to separate the orientational effect of the surrounding molecules on the rotational diffusion of a given chain from the effect of the density on the effective viscosity of the medium.

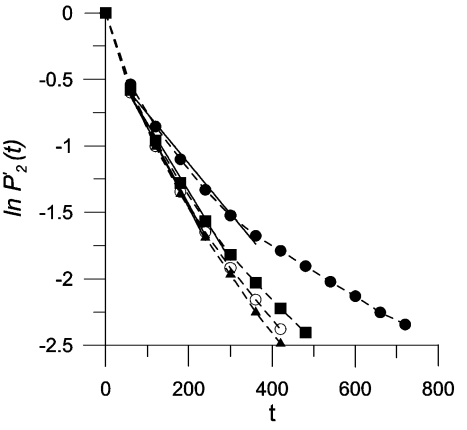

Fig. 12 Logarithm of correlation function $P'_2(t)$ (dashed lines) as a function of time in nematic phase for the system with $l_p = 430$. Circles: $S = 0.909$, squares: $S = 0.885$, open circles: $S = 0.842$, triangles: $S = 0.77$. Solid lines are linear fits used for t_r calculation.

The values of this ratio both for isotropic and nematic phases *versus* S are shown in Fig. 13. It is seen that points corresponding to different l_p in nematic phase fall on a single curve, similar to the case of the anisotropy of translational diffusion (Fig. 9). The universal behavior of the dependences of the rotational mobility on S was observed also in[5] for the nematic phase of colloidal hard spherocylinders exhibiting Brownian dynamics in a solvent. The rotational mobility of particles at relatively small volume fractions was characterized by rates Γ of orientation flips per particle.

It was shown that the values of $\ln\Gamma$ plotted *versus* S for particles with different aspect ratio also fall on a single curve. It is to be noted that in contrast to our systems the viscosity of the solvent in[5] did not change with increase of the volume fraction.

5. Conclusions

The effect of the flexibility on translational and rotational diffusion in the dense systems consisting of semi-flexible molecules has been studied by the molecular dynamics method. For these systems only nematic LC phases were observed. In the isotropic phase the ratio of translational to rotational diffusion coefficients decreases with the decrease of flexibility but remains slightly larger than the theoretical value for a rigid spherocylinder in viscous solvent. In a nematic phase anisotropy of translational diffusion was observed. The diffusion along the nematic director is nonmonotonic in density. The ratio D_{par}/D_{per} of diffusion coefficients parallel and perpendicular to the nematic director plotted *versus* order parameter S fall on a single curve. This result is in agreement with results

Table 3 Values of rotational diffusion coefficient in nematic phase for the systems simulated

l_p	ρ	S	σ_r	t_r	$10^3 D_{rot}^{app}$
132	0.879	0.733	0.108	977.12	0.11
132	0.844	0.675	0.132	794.15	0.16
199.7	0.840	0.832	0.069	593.00	0.12
199.7	0.804	0.814	0.076	390.04	0.19
199.7	0.76	0.762	0.096	357.39	0.27
199.7	0.703	0.578	0.167	438.41	0.38
430.4	0.742	0.909	2.516	264.81	0.13
430.0	0.706	0.885	1.923	194.42	0.24
430.4	0.664	0.842	1.531	171.85	0.37
430.4	0.611	0.77	1.304	164.98	0.58

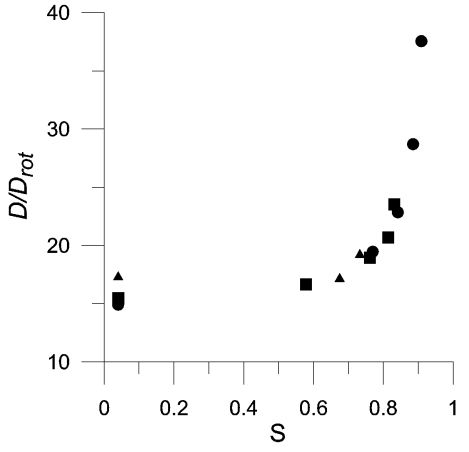

Fig. 13 Ratio D/D_{rot} for isotropic and nematic phases *versus* S for simulated systems. Triangles: $l_{\mathrm{p}} = 132$, squares: $l_{\mathrm{p}} = 199$, circles: $l_{\mathrm{p}} = 430$.

of Lowen[5] for nematic phases of colloidal hard spherocylinders of different aspect ratio in the viscous solvent.

For the estimation of rotational mobility of the molecules in the nematic phase the wobbling-in-a-cone model was used. The ratio of "isotropic" diffusion coefficient to rotational diffusion coefficient *versus* S also fall on a single curve indicating the universal character of this dependence.

In the present work we have simulated anisotropic molecules with the same aspect ratio of 8 in the range of persistence lengths l_{p} between 132 and 430 monomer lengths. It would be interesting to extend this interval to larger l_{p} and aspect ratio.

Acknowledgements

We are very grateful to Professor M. P. Allen for helpful discussion. This paper is a part of the SUPERNET network research of European Science Foundation and INTAS project 99-1114. The financial support from the Academy of Finland is gratefully acknowledged. Russian participants are grateful to the Russian Foundation of Basic Research (grants 02-03-33135 and 99-03-33404).

References

1 L. Onsager, *Ann. NY Acad. Sci.*, 1949, **51**, 627.
2 A. Kolb, PhD Thesis, Mainz, 1999.
3 N. K. Balabaev, A. A. Darinskii, I. M. Neelov, A. Zarembo and F. Sundholm, *J. Polym. Sci. Ser. A*, **44**, 1146.
4 T. Kirchhoff, H. Lowen and R. Klein, *Phys. Rev. E*, 1996, **53**, 5011.
5 H. Lowen, *Phys. Rev. E*, 1999, **59**, 1989.
6 M. P. B. van Bruggen, H. N. W. Lekkerkerker, G. Maret and J. K. G. Dhont, *Phys. Rev. E*, 1998, **58**(6 Part B), 7668.
7 M. P. Allen, *Phys. Rev. Lett.*, 1990, **65**, 2881.
8 S. Hess, D. Frenkel and M. P. Allen, *Mol. Phys.*, 1991, **74**, 765.
9 T. Odijk, *Macromolecules*, 1986, **19**, 2313.
10 A. Yu. Grosberg and A. R. Khokhlov, *Soc. Sci. Rev. A: Phys.*, 1987, **8**, 147.
11 D. Frenkel and B. M. Mulder, *Mol. Phys.*, 1985, **55**, 1171.
12 G. J. Vroege and H. N. W. Lekkerkerker, *Rep. Prog. Phys.*, 1992, **55**, 1241.
13 M. P. Allen and M. R. Wilson, *Mol. Phys.*, 1992, **80**, 277.
14 M. Dijkstra and D. Frenkel, *Phys. Rev. E*, 1995, **51**, 5891.
15 A. Yethiraj and H. Fynewever, *Mol. Phys.*, 1998, **93**, 693.
16 P. Bladon and D. Frenkel, *J. Phys.: Condens. Matter.*, 1996, **8**, 9445.
17 M. P. Allen and D. J. Tildsley, *Computer Simulations of Liquids*, Clarendon, Oxford, 1987, p. 24.
18 H. J. C. Berendsen, J. P. M. Postma and W. F. Gunsteren, *J. Chem. Phys.*, 1984, **81**, 3684.
19 P. J. Flory, *Statistical Mechanics of Chain Molecules*, Interscience Publishers, New York, NY, 1969.
20 M. M. Tirado, C. L. Martinez and J. G. de la Torre, *J. Chem. Phys.*, 1984, **81**, 2047.
21 C. L. Martinez and J. G. de la Torre, *Biophys. J.*, 1987, **52**, 303.